

# $Z^0$ -boson production in association with a top anti-top pair at NLO accuracy with parton shower effects

M. V. Garzelli,<sup>1,2</sup> A. Kardos,<sup>1,3</sup> C. G. Papadopoulos,<sup>4</sup> and Z. Trócsányi<sup>1,3</sup>

<sup>1</sup>*Institute of Physics, University of Debrecen,*

*H-4010 Debrecen P.O.Box 105, Hungary*

<sup>2</sup>*Laboratory for Astroparticle Physics,*

*University of Nova Gorica, SI-5000 Nova Gorica, Slovenia*

<sup>3</sup>*Institute of Nuclear Research of the Hungarian Academy of Sciences, Hungary*

<sup>4</sup>*Institute of Nuclear Physics, NCSR Demokritos GR-15310 Athens, Greece*

(Dated: July 9, 2018)

## Abstract

We present predictions for the production cross section of a Standard Model  $Z^0$ -boson in association with a  $t\bar{t}$  pair at the next-to-leading order accuracy in QCD, matched with shower Monte Carlo programs to evolve the system down to the hadronization energy scale. We adopt a framework based on three well established numerical codes, namely the POWHEG-BOX, used for computing the cross section, HELAC-NLO, which generates all necessary input matrix elements, and finally a parton shower program, such as PYTHIA or HERWIG, which allows for including t-quark and  $Z^0$ -boson decays at the leading order accuracy and generates shower emissions, hadronization and hadron decays.

PACS numbers: 12.38.-t, 13.87.-a, 14.65.Ha, 14.80.Hp

With increasing collider energies, the t-quark plays an increasingly important role in particle physics. Its production cross section grows faster with energy than that of any other discovered Standard Model (SM) particle. Already after the first year of successful run of the LHC, the  $t\bar{t}$  production cross section is measured with unprecedented accuracy at  $\sqrt{s} = 7\text{ TeV}$ , so that the corresponding SM theoretical prediction will be challenged soon [1, 2]. However, many other t-quark properties have not yet been directly accessed. In particular, its couplings to neutral gauge (especially the  $Z^0$ ) and scalar bosons are still prone to large uncertainties. In Refs. [3, 4] the possibility of measuring the  $t\bar{t}Z$  and  $t\bar{t}\gamma$  couplings was studied based upon leading-order (LO) parton level predictions. Although such precision is sufficient for feasibility studies, finding the optimal values of the experimental cuts requires indeed predictions at higher accuracy.

An essential step towards higher accuracy is the inclusion of next-to-leading order (NLO) radiative corrections. Recent theoretical advances made possible our computation of the  $pp \rightarrow t\bar{t}Z$  cross section at the parton level, including QCD corrections at NLO [5]. In order though to get the optimum benefit and to produce predictions that can be directly compared to experimental data at the hadron level, a matching with parton shower (PS) and hadronization implemented in shower Monte Carlo (SMC) programs is ultimately inevitable. Thus, in this letter we present first predictions for  $pp \rightarrow t\bar{t}Z$  production at LHC at the matched NLO + PS accuracy.

In constructing a general interface of PS to matrix element (ME) computations with NLO accuracy in QCD, we have chosen to combine the POWHEG [6, 7] method and FKS subtraction scheme [8], as implemented in the POWHEG-BOX [9] computer framework, with the HELAC-NLO [10] approach, respectively. In particular, POWHEG-BOX requires the relevant MEs as external input. We obtain the latter in a semi-automatic way by codes in the HELAC-NLO package [11]. With this input POWHEG-BOX is used to generate events at the Born plus first radiation emission level, stored in Les Houches Event Files (LHEF) [12], that can be interfaced to standard SMC programs. Previous applications of the whole framework, proving its robustness, were presented in Refs. [13, 14]. This same setup also allows for exact NLO pure hard-scattering predictions. Further details on the implementation of the computation of the  $pp \rightarrow t\bar{t}Z$  hard-scattering cross-section in it, at NLO accuracy in QCD, together with checks, were recorded in Ref. [5].

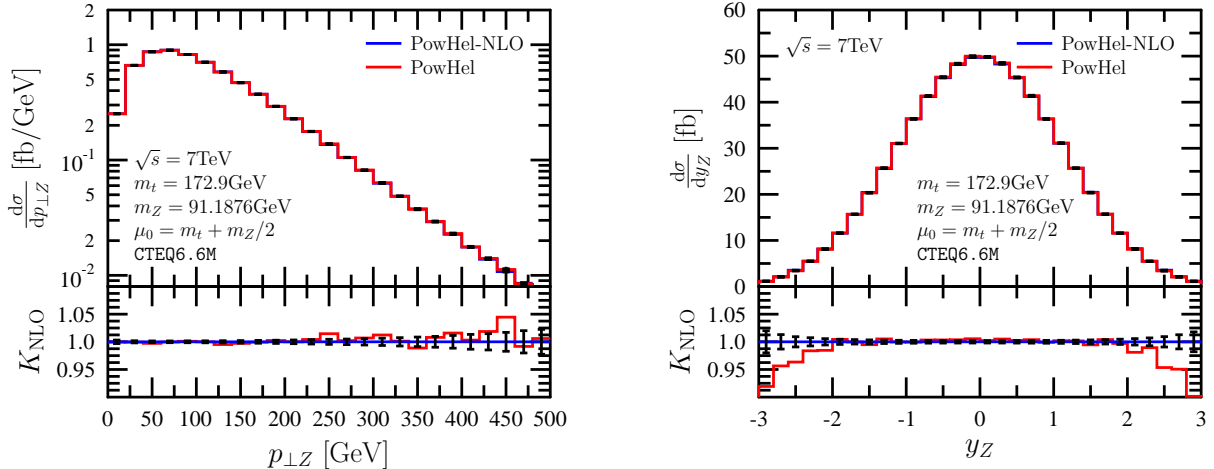


Figure 1. Transverse momentum (left) and rapidity (right) distributions of the  $Z^0$ -boson at NLO and after first radiation (PowHel). The lower panels show the ratio of the two predictions with combined uncertainties.

All these computations are steps of an ongoing project for generating event samples for  $pp \rightarrow t\bar{t}X$  processes, where  $X$  stays for a hard partonic object. The events we generate are stored in LHEF, made available on the web, and are ready to be interfaced to standard SMC programs to produce predictions for distributions at the hadron level. Such predictions can be useful for optimizing the selection cuts applied to disentangle the signal from the background, in order to improve the experimental accuracy of the t-quark coupling measurements.

Interfacing NLO calculations to SMC programs allows to estimate the effects of decays, shower emissions and hadronization, therefore we have analyzed the process at hand at three different stages of evolution:

**PowHel:** we analyzed the events including no more parton emissions than the first and hardest one, collected in LHEF produced as output of POWHEG-BOX+ HELAC-NLO (PowHel).

**Decay:** we just included on-shell decays of t-quarks and the  $Z^0$ -boson, as implemented in PYTHIA [15], and further decays of their decay products, like charged leptons (the  $\tau$  is considered as unstable) and gauge bosons ( $W$ ), turning off any initial and final PS and hadronization effect.

**Full SMC:** decays, shower evolution, hadronization and hadron decays have been included in our simulations, using both `PYTHIA` and `HERWIG` [16].

In our computation, we adopted the following parameters:  $\sqrt{s} = 7 \text{ TeV}$ , `CTEQ6.6M` PDF set from `LHAPDF`, with a 2-loop running  $\alpha_s$ , 5 light flavours and  $\Lambda_5^{\overline{\text{MS}}} = 226 \text{ MeV}$ ,  $m_t = 172.9 \text{ GeV}$ ,  $m_Z = 91.1876 \text{ GeV}$ ,  $G_F = 1.16639 \cdot 10^{-5} \text{ GeV}^{-2}$ . The renormalization and factorization scales were chosen equal to the default scale  $\mu_0 = m_t + m_Z/2$ . We used the last version of the SMC fortran codes: `PYTHIA 6.425` and `HERWIG 6.520`. Following our implementation of  $t\bar{t}H$  hadroproduction in Ref. [14], in both SMC setup muons (default in `PYTHIA`) and neutral pions were assumed as stable particles. All other particles and hadrons were allowed to be stable or to decay according to the default implementation of each SMC. Masses and total decay widths of the elementary particles were tuned to the same values in `PYTHIA` and `HERWIG`, but each of the two codes was allowed to compute autonomously partial branching fractions in different decay channels for all unstable particles and hadrons. Multiparticle interaction effects were neglected (default in `HERWIG`). Additionally, the intrinsic  $p_{\perp}$ -spreading of valence partons in incoming hadrons in `HERWIG` was assumed to be  $2.5 \text{ GeV}$ .

First, to check event generation, we compared several distributions from events including no more than first radiation emission (`PowHel` level) with the NLO predictions of Ref. [5]. We found agreement for all considered distributions. As examples, we show in Fig. 1 the transverse momentum and rapidity distributions of the  $Z^0$ -boson.

Next, we studied the effect of the full SMC by comparing distributions at the decay and SMC level. Since particle yields are very different at the end of these two stages, we made such a comparison without any selection cut, in order to avoid the introduction of any bias. As an illustrative example, we present the distributions of the transverse momentum and rapidity of the hardest jet,  $p_{\perp}^j$  and  $y_j$ , in Fig. 2. Jets are reconstructed through the anti- $k_{\perp}$  algorithm with  $R = 0.4$ , as implemented in `FastJet` [17]. The softening of the transverse momentum spectrum is apparent as going from the decay level to the full SMC one, while the effect of the shower on the rapidity of the hardest jet is almost negligible and rather homogeneous. The cross-section at both level amounts to  $\sigma = 138.7 \pm 0.01 \text{ fb}$ . Using our setup for the full SMC's, we found agreement between `PYTHIA` and `HERWIG` predictions within very few percent, despite the conceptual differences between the two SMC generators as for the shower ordering variables and hadronization models, confirming the level of agreement

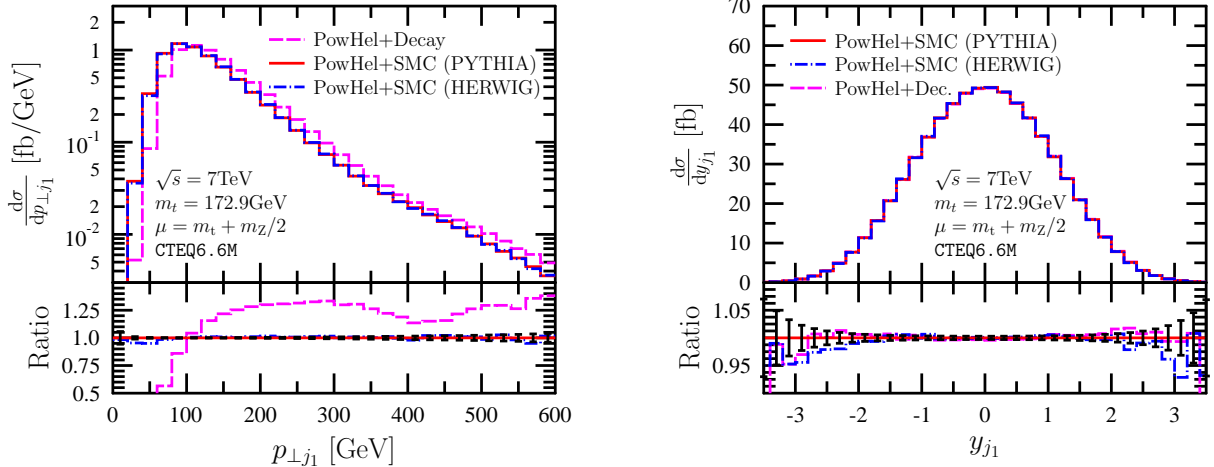


Figure 2. Transverse momentum (left) and rapidity (right) distributions of the hardest jet after decay and after full SMC. The lower panels show the ratio of all predictions to PowHel+SMC using PYTHIA.

already reported in Ref. [14] in the study of a different process.

Next, we made predictions for  $t\bar{t}Z$  hadroproduction at the LHC including experimental selection cuts. For this analysis, in the absence of a dedicated tune for NLO matched computations, PYTHIA was tuned to the Perugia 2011 set of values, one of the most recent LO tunes [18], updated on the basis of recent LHC data, providing a  $p_{\perp}$ -ordered PS. Its application turned out to increase our particle yields by about 10%. As a consequence, the agreement between the tuned PYTHIA and untuned HERWIG predictions decreases (as for HERWIG, the default configuration was used, providing instead an angular-ordered PS), and we present only the PYTHIA ones.

In case of  $t\bar{t}Z$  hadroproduction overwhelming backgrounds come from  $t\bar{t}$ +jets final states. In Ref. [4] the differential cross section as a function of missing transverse momentum for the production of  $p_{\perp}b\bar{b}+4$  jets was found a useful tool for differentiating the signal and the possible backgrounds. The proposed set of selection cuts is rather exclusive and the rates decrease so much that the measurement for the present LHC run at  $\sqrt{s} = 7$  TeV looks quite demanding from the statistical point of view, therefore, we restrict ourself to present predictions for the future runs at  $\sqrt{s} = 14$  TeV ( $\sigma_{\text{all cut},14}/\sigma_{\text{all cut},7} \sim 7$  and 8 at the decay and at the full SMC level, respectively).

In Fig. 3 we show the distributions of transverse momentum and rapidity of the hardest

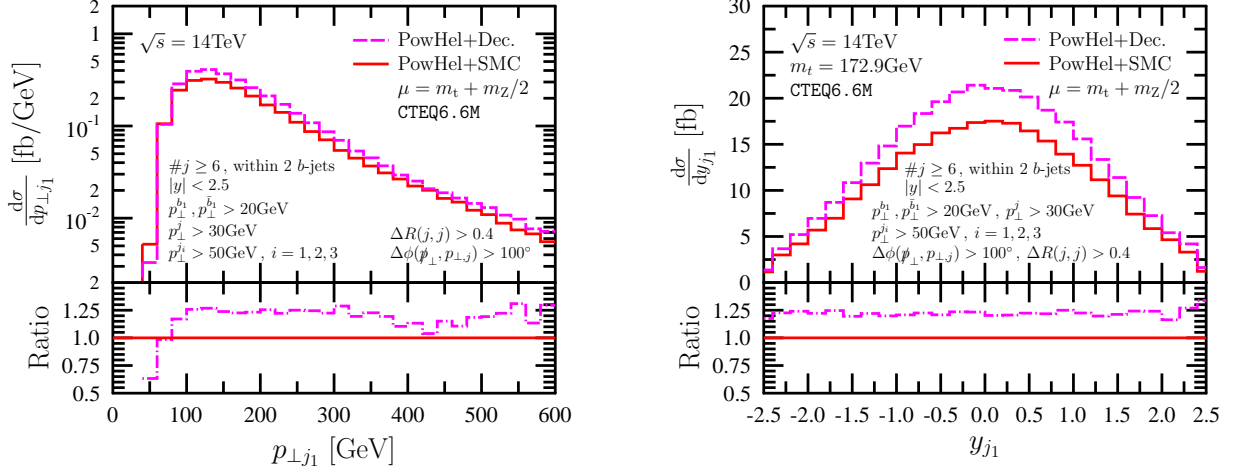


Figure 3. Transverse momentum (left) and rapidity (right) distributions of the hardest jet after decay and after full SMC (PYTHIA), under selection cuts (1–8) implemented at both levels. The lower panels show the ratio of the predictions at different levels.

jet using the following reduced set of cuts: 1) we reconstruct at least six jets with rapidity  $|y| < 2.5$ , 2) of these we require at least one  $b$ -jet and one  $\bar{b}$ -jet, 3) for  $b$ -jets  $p_{\perp}^b > 20$  GeV, 4) for other jets  $p_{\perp}^{\text{non } b} > 30$  GeV, 5) at least 3 jets ( $b$  or non- $b$ ) with  $p_{\perp}^j > 50$  GeV, 6)  $\Delta R(j, j) > 0.4$ , where  $j$  denotes any ( $b$  or non- $b$ ) jet and  $\Delta R$  is defined as  $\sqrt{\Delta\phi^2 + \Delta y^2}$ , 7–8)  $\Delta\phi(\hat{p}_{\perp}, p_{\perp, j}) > 100^\circ$ , with  $p_{\perp, j}$  meaning either  $(p_{\perp}(\hat{b}_1) + p_{\perp}(\hat{b}_2))$  (cut 7), or  $(p_{\perp}(\hat{j}_1) + p_{\perp}(\hat{j}_2) + p_{\perp}(\hat{j}_3) + p_{\perp}(\hat{j}_4))$  (cut 8), where  $\hat{b}_1, \hat{b}_2$  and  $\hat{j}_1, \hat{j}_2, \hat{j}_3, \hat{j}_4$  are the jets that allow for the best  $t \rightarrow bW^+ \rightarrow bj\bar{j}$  and  $\bar{t} \rightarrow \bar{b}W^- \rightarrow \bar{b}j\bar{j}$  invariant mass simultaneous reconstruction, since they minimize the

$$\chi^2(b_1 j_1 j_2; \bar{b}_2 j_3 j_4) = \frac{(m_{j_1 j_2} - m_W)^2}{\sigma_W^2} + \frac{(m_{j_3 j_4} - m_W)^2}{\sigma_W^2} + \frac{(m_{b_1 j_1 j_2} - m_t)^2}{\sigma_t^2} + \frac{(m_{\bar{b}_2 j_3 j_4} - m_t)^2}{\sigma_t^2}$$

computed by considering all possible  $j_k j_l$ ,  $b_i j_k j_l$  and  $\bar{b}_i j_k j_l$  combinations. The  $W \rightarrow j\bar{j}$  and  $t \rightarrow bj\bar{j}$  invariant mass resolutions were set to  $\sigma_W = 7.8$  GeV and  $\sigma_t = 13.4$  GeV, respectively [19]. The PowHel+PYTHIA cross sections after these cuts amount to  $\sigma_{\text{dec}} = 65.56 \pm 0.15$  fb and  $\sigma_{\text{SMC}} = 53.74 \pm 0.13$  fb.

In Fig. 4 we plot the invariant mass distribution of the  $t$ -quark, as reconstructed from its decay products, by minimizing the  $\chi^2$  above. At the decay level, the reconstruction leads to a clear peak centered around the  $m_t$  value. On the other hand, after full SMC, due both to

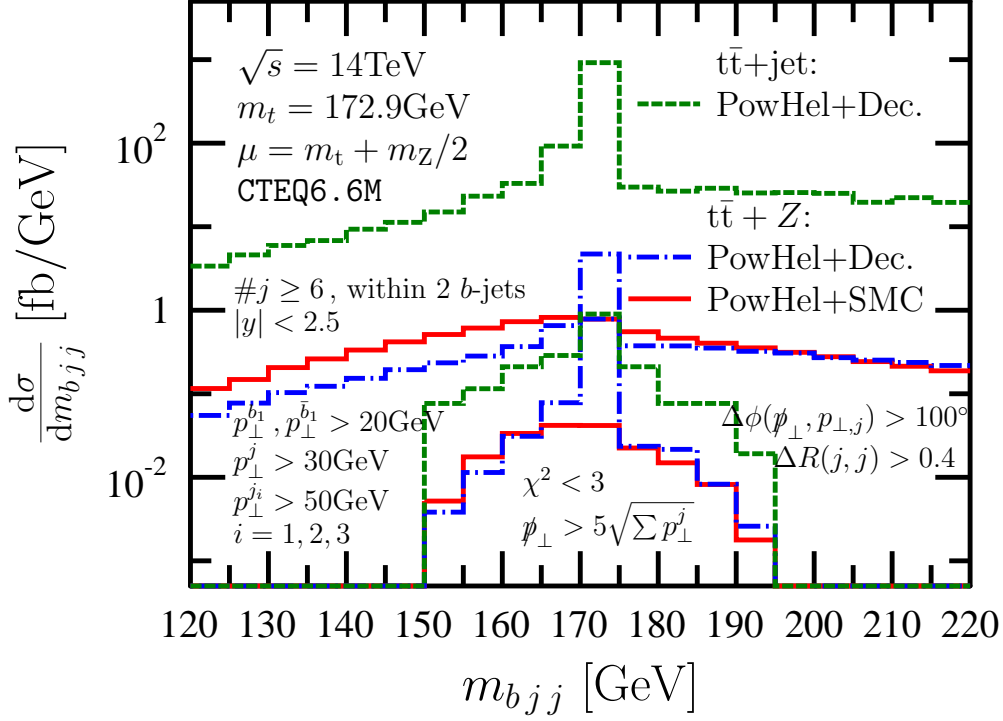


Figure 4. Invariant mass distribution of the  $t$ -quark reconstructed from the decay products at both decay and full SMC levels, for the  $t\bar{t}Z$  signal and, at the decay level, for one background ( $t\bar{t}$ +jet) after selection cuts (1–8) (wider distributions in abscissa values) and after selection cuts (1–10) (narrower distributions).

further emissions which modify jet content and to hadron decays, there are more candidate jets and the reconstruction is less successful. Although a peak is still visible (more evident in non-log scale), it is smeared towards lower mass values. The effect of the shower and hadronization turns out to be especially large in the peak region.

In Fig. 4 we also show the  $m_{bjj}$  distribution after decay for an important background process:  $t\bar{t}$ -pair production associated with a jet (obtained at the scale  $\mu_0 = m_t$ ). Clearly, the background overwhelms the signal, therefore, in order to select the peak region, we include two more cuts: 9)  $p_{\perp}$  (due to all  $\nu$ 's)  $> 5\sqrt{\sum p_{\perp}^j}$  (of all jets,  $b$  or non- $b$ ), and 10)  $\chi_{\min}^2 < 3$ , where  $\chi_{\min}^2$  is the minimum of the  $\chi^2$  above. Thus, we closely reproduce the cuts in Ref. [4], aimed at favoring the  $Z^0 \rightarrow \nu\nu$  decay channel. The effect of the whole set of

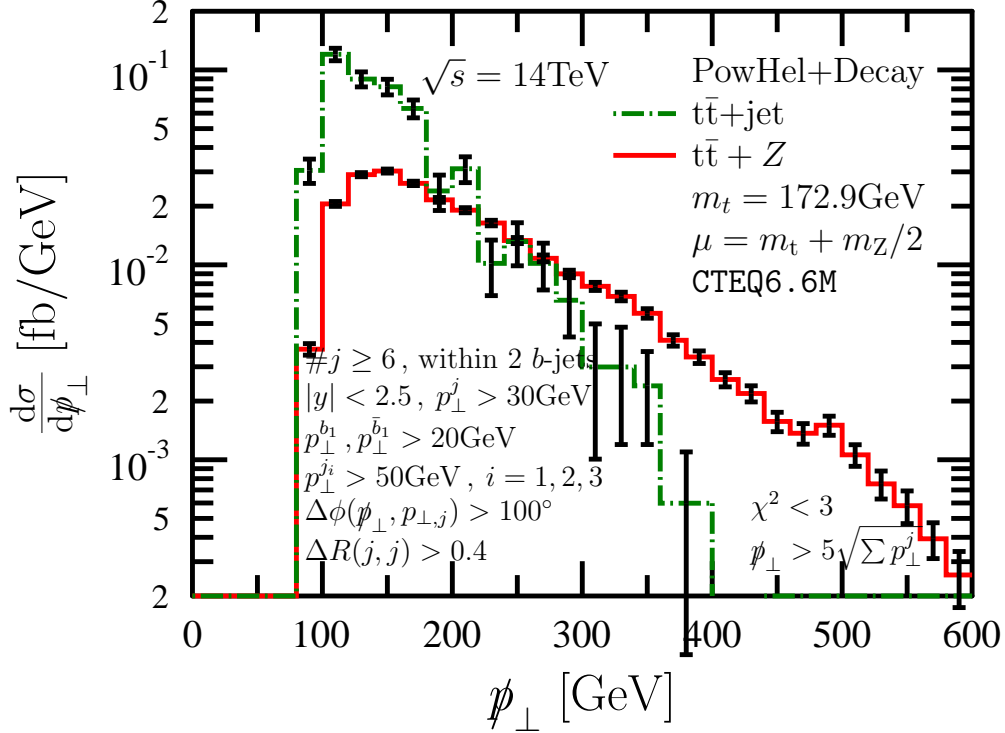


Figure 5. Distribution of the missing transverse momentum after decay, under physical cuts (1–10) applied to the signal ( $t\bar{t}Z$ ) and to one background ( $t\bar{t}+\text{jet}$ ).

cuts on top reconstruction in  $t\bar{t}Z$  and  $t\bar{t}+\text{jet}$  events is also shown in Fig. 4. Although this set of cuts is effective in selecting the signal, the background is globally still larger: for the signal  $\sigma_{\text{dec}} = 4.83 \pm 0.04 \text{ fb}$ , while for the background  $\sigma_{\text{dec}} = 9.86 \pm 1.05 \text{ fb}$ . However, as can be understood from Fig. 5, where the distributions of the missing transverse momentum after decay are shown for both  $t\bar{t}Z$  and  $t\bar{t}+\text{jet}$ , these cuts allow for disentangling the signal, at least at the decay level. At the shower level, the  $p_{\perp}$  distributions of the  $t\bar{t}Z$  signal still shows a harder spectrum than the one of the  $t\bar{t}+\text{jet}$  background, but to a lesser extent. In this case, the effect of different top reconstruction strategies, still under investigation, can be crucial to help better disentangle the signal from the background in the  $p_{\perp} b\bar{b}+4$  jets considered channel.

We studied the hadroproduction of a  $Z^0$  boson in association with a  $t\bar{t}$ -pair, process of interest for measuring the  $t\bar{t}Z$ -coupling directly at the LHC. We studied the effect of heavy



particle decays as well as the one of the full SMC. We produced predictions for the LHC. As the production cross section is rather small, measuring the  $t\bar{t}Z$ -coupling becomes more feasible after the planned 14 TeV energy upgrade. Once all background processes will be predicted with the same accuracy, our predictions will make possible a realistic optimization of the experimental cuts.

This research was supported by the HEPTOOLS EU program MRTN-CT-2006-035505, the LHCPheNet network PITN-GA-2010-264564, the Swiss National Science Foundation Joint Research Project SCOPES IZ73Z0\_1/28079, the TÁMOP 4.2.1./B-09/1/KONV-2010-0007 project, the Hungarian Scientific Research Fund grant K-101482, the MEC project FPA 2008-02984 (FALCON). M.V.G and Z.T thank the Galileo Galilei Institute for Theoretical Physics for the hospitality and the INFN partial support. We are grateful to A. Tropiano, G. Dissertori, S. Moch and P. Skands for discussions.

- 
- [1] M. Saleem, arXiv:1109.3912.
  - [2] S. Chatrchyan *et al.* [CMS Collaboration], Phys. Rev. D **84**, 092004 (2011) [arXiv:1108.3773].
  - [3] U. Baur, A. Juste, L. H. Orr and D. Rainwater, Phys. Rev. D **71**, 054013 (2005) [arXiv:hep-ph/0412021].
  - [4] U. Baur, A. Juste, D. Rainwater and L. H. Orr, Phys. Rev. D **73**, 034016 (2006) [arXiv:hep-ph/0512262].
  - [5] A. Kardos, C.G. Papadopoulos and Z. Trócsányi, arXiv:1111.0610.
  - [6] P. Nason, JHEP **0411**, 040 (2004) [arXiv:hep-ph/0409146].
  - [7] S. Frixione, P. Nason and C. Oleari, JHEP **0711**, 070 (2007) [arXiv:0709.2092].
  - [8] S. Frixione, Z. Kunszt, A. Signer, Nucl. Phys. B **467**, 399 (1996) [arXiv:hep-ph/9512328].
  - [9] S. Alioli, P. Nason, C. Oleari and E. Re, JHEP **1006**, 043 (2010) [arXiv:1002.2581].
  - [10] G. Bevilacqua *et al.*, Nucl. Phys. Proc. Suppl. **205-206**, 211 (2010) [arXiv:1007.4918].
  - [11] G. Bevilacqua *et al.*, arXiv:1110.1499.
  - [12] J. Alwall *et al.*, Comput. Phys. Commun. **176**, 300 (2007) [arXiv:hep-ph/0609017].
  - [13] A. Kardos, C. Papadopoulos and Z. Trócsányi, Phys. Lett. B **705**, 76 (2011) [arXiv:1101.2672].
  - [14] M. V. Garzelli, A. Kardos, C. G. Papadopoulos and Z. Trócsányi, Europhys. Lett. **96**, 11001 (2011) [arXiv:1108.0387].

- [15] T. Sjostrand, S. Mrenna and P. Z. Skands, JHEP **0605**, 026 (2006) [arXiv:hep-ph/0603175].
- [16] G. Corcella *et al.*, arXiv:hep-ph/0210213.
- [17] M. Cacciari, G. P. Salam and G. Soyez, JHEP **04**, 063 (2008) [arXiv:0802.1189].
- [18] P. Z. Skands, Phys. Rev. D **82**, 074018 (2010) [arXiv:1005.3457].
- [19] M. Beneke *et al.*, arXiv:hep-ph/0003033.